One-step Fabrication of Nickel Hierarchical Superstructures

Zhe Chen, Minhua Cao,* and Xiaoyan He
Department of Chemistry, Northeast Normal University, Changchun 130024, P. R. China

(Received March 26, 2008; CL-080320; E-mail: caomh043@nenu.edu.cn)

Nickel hierarchical superstructures have been successfully produced via a simple surfactant-assisted hydrothermal method. The resulting superstructures are formed by the self-assembly of sea urchin-shaped microspheres. Here, poly(vinylpyrrolidone) (PVP) plays an important role in the formation of such structures. A feasible formation mechanism was proposed. The magnetic measurement suggests that the nickel superstructures exhibit ferromagnetic behavior at room temperature.

In the past few years, the assembly of three-dimensional (3D) hierarchical superstructures has attracted considerable attention in the area of materials science because of their widespread and potential applications in electronic, magnetic, and optical devices.[1,2] Generally, materials with different superstructures may exhibit different physical and chemical properties because of their complexity of possible arrangement. Various strategies, such as laser-assisted catalytic growth, template-based techniques, vapor–liquid–solid reaction, and solution-based self-assembly routes, have been developed for hierarchical assembly.[3] In these approaches, it is obvious that the solution-based routes that combine synthesis with in situ assembly are highly desired for their simplicity and for the novel structures that often formed. Studies have shown in the past few years that under certain solution conditions, some special and novel superstructures, that can not be formed using other methods, could be spontaneously obtained in a one-step reaction.[4] Therefore, the development of simple, facile, and effective solution methods for the hierarchical assembly over multiple length scales are particularly promising for designing functional nanostructures and assembling nanoscale devices.

Recently, control over the fabrication and assembly of metal nanostructures have received extraordinary interest because of their important potential in applications, such as photonics, electronics, magnetism, catalysis, optics, optoelectronics, pigments, elements of chemical and biological sensors, information storage, and so on.[5] Among these metal nanostructures, magnetic materials have attracted particular interest because of their extensive applications including high-density magnetic recording, magnetic sensors, superparamagnetism, magnetic dipolar interactions, and magnetoresistance.[5c] More recently, a new trend of exploring various shapes of nickel-based nanomaterial has emerged because of their important properties, catalysts, components of magnetic data storage media, and biological sensors. Accordingly, various strategies have been developed to prepare nickel nanomaterials. For example, Qian et al. prepared nickel nanobelts relying on the presence of complex-surfactant-assisted hydrothermal method,[6] Cai et al. prepared nickel nanorings and hollow sphere arrays by morphology inheritance based on ordered through-pore template and electrodeposition,[7] and Chen et al. reported the production of one-dimensional self-assembling of acicular nickel nanocrystallites under the magnetic field conditions.[8] Many other various anisotropic nanostructures have also been produced, including nanoplatelets,[9] nanosheets,[10] nanorods,[11] nanoflowers,[12] and hollow spheres.[13] However, no reports have been focused on the fabrication of nickel hierarchical superstructures. The development of mild, facile, and effective methods for producing such structures is a major challenge. Herein, we report the first example of 3D hierarchical superstructures, self-assembled by sea urchin-like structures, by using PVP-assisted hydrothermal process, which provides a one-step fabrication of hierarchical superstructures.[14]

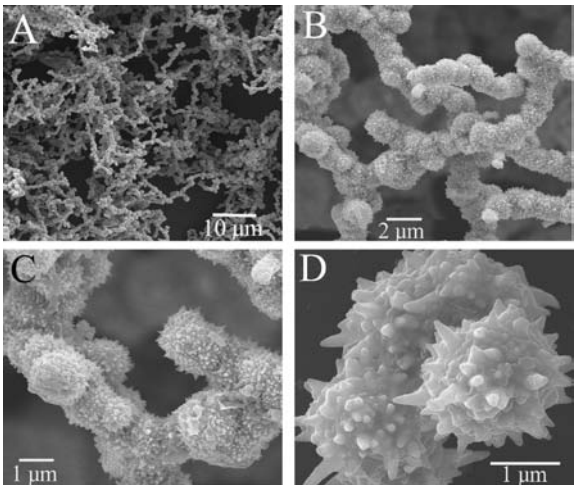

Figure 1. SEM images of nickel sample at different magnifications (A)–(D).

Figure S1[14] shows the X-ray powder diffraction (XRD) pattern of an as-prepared nickel sample. All of the peaks can be assigned to the cubic nickel phase (JCPDS No. 04-0850). A trace amount PVP is still found to be included in the sample from the FTIR spectrum (Figure S2),[14] although it has not been detected in the XRD pattern. Figure 1 shows the SEM images of the nickel sample with different magnifications. An overview image with a low magnification (Figure 1A) reveals that the sample exhibits a 3D network superstructure. A detailed views of the product (Figures 1B–1D) show that this superstructure is formed by the self-assembly of some microparticles with a sea urchin shape, which consist of the core with a diameter of 1–2 μm and the conical nanolobes with different lengths. Figures 2A and 2B show the TEM images of nickel sample, which further confirm its superstructures and the sea urchin shape of the individual building block. Figure 2C is the high-resolution TEM image of the tip of a conical nanolobe. It can be seen that it exhibits clear two-dimensional lattice, suggesting the single-crystal nature of the conical nanolobe segment. Figure 2D shows a selected-area electron diffraction (SAED) pattern from a single sea urchin-shaped microparticle. The SAED pattern with the rings comprising of clear diffraction spots can be unambiguously attributed to the fact that the sea urchin-shaped microparticles are polycrystalline and are composed of large individual crystals.

To learn more about the effect of PVP on nickel superstructures, a series of experiments with different concentrations of PVP or in the absence of PVP have been carried out. When no PVP was used in the reaction system, only irregular particles with no sea urchin-shaped structures were obtained, as shown in Figure S3.[14] With the addition of 0.006 M PVP in the reaction sys-

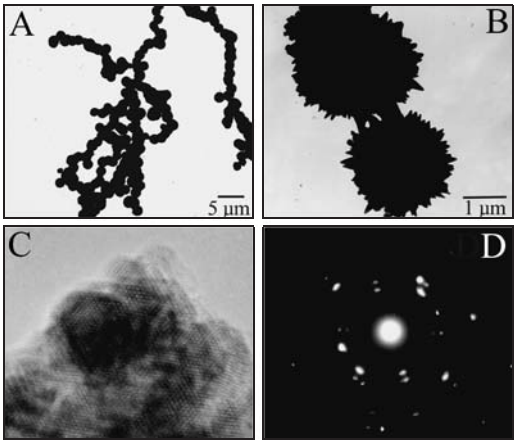

Figure 2. (A) TEM image nickel sample at low magnification. (B) TEM image nickel sample at large magnification. (C) HRTEM image, (D) SAED image of nickel sample.

tem, 3D superstructures self-assembled by the aggregation of sea urchin-shaped nanoparticles were formed, as shown in Figure 1. When the concentration of PVP was increased to 0.012 and 0.018 M, 3D superstructures could be obtained, but the conical nanolobes of the sea urchin-shaped nanoparticles became shorter (see Figures S3B and S3C).[14] So, it can be clearly seen that PVP plays an important role in the formation of the perfect 3D hierarchical superstructures. Recently, our group has prepared many nanomaterials by means of surfactants as structure-directed agents. A series of studies indicated that the morphology of the final products strongly depends on the kind of surfactant.[15a]

To elucidate the formation mechanism of above hierarchical superstructures, the growth of particles was monitored as a function of reaction time. It was found that the formation of the hierarchical superstructures is a typical Ostwald ripening process (crystallites grow at the expense of the small ones).[15b] As shown in Figure 3A, when reaction time was 4 h, nanoparticles with an average diameter of 400 nm were observed in the presence of PVP. After 8 h, some larger round-like particles were formed at the expense of small particles and some of the particles are "fused" together forming elongated aggregates (Figure 3B). As the reaction was prolonged to 16 h, the amount of small particles was largely reduced and the aggregates consisting of round-like particles became longer (Figure 3C). When the reaction time was changed to 18 h, small nanoparticles depleted and original smooth particles were transformed into sea urchin-shaped microparticles (Figure 3D). The reason may be that the surfaces of the smooth particles serve as nucleation sites and that conical nanolobes were formed on their surfaces. When the reaction time finally reached 24 h, well-defined 3D hierarchical superstructures were observed.

The magnetic properties of nickel superstructures were investigated by recording both the temperature-dependent magnetization and hysteresis curves, as shown in Figure 4. It clearly reveals typical ferromagnetic behaviors. Figure 4 (M–T curves) is

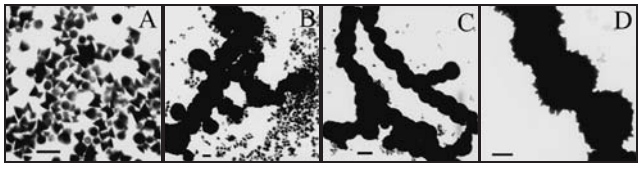

Figure 3. TEM images of samples obtained with different reaction times (scale bar = 400 nm) (a) 4 h; (b) 8 h; (c) 12 h; (d) 18 h.

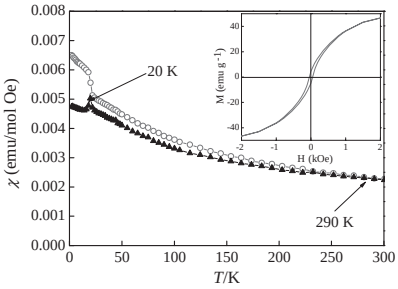

Figure 4. The dependence of ZFC and FC on temperature of nickel sample. Both the cooling and measurement external magnetic fields are 50 Oe, inset shows M–H loops of nickel sample measured at 300 K.

composed of zero-field-cooled (ZFC) and field-cooled (FC) curves. The existence of a sharp peak at ≈20 K in ZFC, which corresponds to the blocking temperature (T_B) value of hcp Ni nanoparticles, may be explained by a trace amount of hcp Ni in the sample.[16] The broad peak at about 290 K can be ascribed to the T_B of fcc Ni superstructures, suggesting ferromagnetic characteristics of as-prepared nickel superstructures almost at room temperature. This behavior is similar to the bulk one.[13] The hysteresis loop (inset in Figure 4) of this material measured at 300 K further confirms its ferromagnetic behavior with a coercive force (Hc) of 48.4 Oe. By comparing the coercive force with that of the bulk one at room temperature (ca. 0.7 Oe),[13] it can be clearly seen that the present sample exhibits an enhanced coercive force, which is probably attributed to the shape anisotropy of nickel superstructures.

In summary, we have successfully made nickel 3D superstructures under hydrothermal conditions. It was found that PVP plays an important role in the formation of these superstructures. Furthermore, its magnetic properties are very interesting and could be potentially applicable to many important fields in the future. This method can be further applied to the preparation of other related materials.

The authors thank the National Natural Science Foundation of China (NSFC, No. 20771022), the Huo Yingdong Foundation, and Analysis and Testing Foundation of Northeast Normal University for financial support.

References and Notes

1 S.-H. Yu, M. Antonietti, H. Colfen, J. Hartman, *Nano Lett.* **2003**, *3*, 379.
2 Z. L. Wang, *J. Phys. Chem. B* **2000**, *104*, 1153.
3 a) J. Y. Lao, J. G. Wen, Z. F. Ren, *Nano Lett.* **2002**, *2*, 1287. b) A. M. Morales, C. M. Lieber, *Science* **1998**, *279*, 208. c) S. Mann, G. A. Ozin, *Nature* **1996**, *382*, 313.
4 H.-P. Liang, H.-M. Zhang, J.-S. Hu, Y.-G. Guo, L.-J. Wan, C.-L. Bai, *Angew. Chem., Int. Ed.* **2004**, *43*, 1540.
5 a) T. Hyeon, *Chem. Commun.* **2003**, 927. b) L. Guo, Q. Huang, X.-Y. Li, S. Yang, *Phys. Chem. Chem. Phys.* **2001**, *3*, 1661. c) X. Teng, H. Yang, *J. Am. Chem. Soc.* **2003**, *125*, 14559.
6 Z. Liu, S. Li, Y. Yang, S. Peng, Z. Hu, Y. Qian, *Adv. Mater.* **2003**, *15*, 1946.
7 G. Duan, W. Cai, Y. Luo, Z. Li, Y. Lei, *J. Phys. Chem. B* **2006**, *110*, 15729.
8 H. Niu, Q. Chen, M. Ning, Y. Jia, X. Wang, *J. Phys. Chem. B* **2004**, *108*, 3996.
9 J. Li, Y. Qin, X. Kou, J. Huang, *Nanotechnology* **2004**, *15*, 982.
10 Y. Leng, Y. Zhang, T. Liu, M. Suzuki, X. Li, *Nanotechnology* **2006**, *17*, 1797.
11 N. Cordente, M. Respaud, F. Senocq, M.-J. Casanove, C. Amiens, B. Chaudret, *Nano Lett.* **2001**, *1*, 565.
12 X. Ni, Q. Zhao, H. Zheng, B. Li, J. Song, D. Zhang, X. Zhang, *Eur. J. Inorg. Chem.* **2005**, 4788.
13 Q. Liu, H. Liu, M. Han, J. Zhu, Y. Liang, Z. Xu, Y. Song, *Adv. Mater.* **2005**, *17*, 1995.
14 Supporting Information is available electronically on the CSJ-Journal Web site, http://www.csj.jp/journals/chem-lett/.
15 a) M. Cao, C. Hu, E. Wang, *J. Am. Chem. Soc.* **2003**, *125*, 11196. b) W. Ostwald, *Z. Phys. Chem.* **1900**, *34*, 495.
16 Y. T. Jeon, J. Y. Moon, G. H. Lee, J. Park, Y. M. Chang, *J. Phys. Chem.* **2006**, *110*, 1187.

Published on the web (Advance View) June 7, 2008; doi:10.1246/cl.2008.736